ELSEVIER

Journal of Nuclear Materials 295 (2001) 157–166

journal of nuclear materials

www.elsevier.nl/locate/jnucmat

Annealing of hardening in copper after neutron irradiation hardening at 77 K

H.C. González *, M.T. Miralles

Departamento Materiales, Centro Atómico Constituyentes, Comisión Nacional de Energía Atómica, Av. del Libertador 8250, Buenos Aires (1429) Argentina

Received 18 August 2000; accepted 20 March 2001

Abstract

The stress–strain curves corresponding to single crystals of Cu irradiated and measured at 77 K revealed the onset of an upper and a lower yield point at fluences higher than 0.5×10^{21} n m^{-2} ($E > 0.5$ MeV), which will be referred to as the critical fluence, $(\phi t)_C$. The lower yield point is associated to the channeling dislocation phenomenon. The upper yield point is taken as the actual yield stress. The isochronal recovery of the critical resolved shear stress (CRSS) around Stage V ($T > 450$ K) in crystals irradiated at 300 K at fluences higher than $(\phi t)_C$, and at 77 K at fluences close to $(\phi t)_C$, was studied in the present work. For both conditions, the presence of a broad recovery stage between 500 and 650 K (Stage V) was determined. In the second case, the presence of three inflections in the isochronal recovery of the CRSS (measured at 77 K), in the temperature sub-ranges: ~490–520; ~520–560 and ~560–620 K was observed.

PACS: 61.80.Hg; 61.82.Bg

1. Introduction

Neutron irradiation in metals produces vacancy and interstitial clusters. These defect clusters act as barriers to dislocation movement, giving rise to a substantial increase in the yield stress [1–3]. The value of the critical resolved shear stress (CRSS) is representative of the clusters present in the lattice [4–10]. This value in single crystals of Zn increases about 5000% when irradiated with fast neutrons at 77 K and 0.5×10^{21} n m^{-2} [11,12]. However, electrical resistivity increases only about 60% [13].

At low irradiation temperatures, the vacancy loops originated at the end of the atomic displacement cascades (ADCs) are the dominant type of defects present [14–25]. At 77 K, only the self-interstitial atoms are considered to be able to migrate, while the vacancies remain immobile [26]. The defect cluster size is nearly independent of fluence in Cu irradiated near room temperature [27–29].

For higher irradiation temperatures, the migration of point defects favors the growth of interstitial loops and the total point defect concentration is thus lower [27,28].

The isochronal annealing of metals irradiated by neutrons at low temperature (4.2 K) usually shows five recovery stages. Each one is associated to the annealing of different defects [30–34]. The recovery of the CRSS takes place mostly in the last stage, or Stage V [35]. It should be emphasized that Stage V in Zn irradiated at low fluences (~0.5×10^{21} n m^{-2}) at 77 K, was resolved by the isochronal recovery of hardening [36] but not by resistivity measurements [37]. In Cu, as opposed to Stages I and III [30–34,38,39], Stage V ($T > 450$ K) has been scarcely studied [25,40–42]. This stage is associated with the dissolution of vacancy loops, which were originated in the depleted zones at the end of the cascades produced during neutron irradiation [2,20,32]. From isothermal and isochronal annealing studies of the CRSS in irradiated copper with fission reactor neutrons, an activation energy similar to that for vacancies

* Corresponding author. Tel.: +54-11 4754 7445/7352; fax: +54-11 4754 7362.

E-mail addresses: hecgonza@cnea.gov.ar (H.C. González), miralles@cnea.gov.ar (M.T. Miralles).

0022-3115/01/$ - see front matter
PII: S0022-3115(01)00559-1

self-diffusion (2–2.5 eV) is usually associated with the middle part of Stage V, the activation energy being an increasing function of temperature in the involved range [1,26,34,43–46].

In studies by TEM the accumulation of defect at elevated temperatures [25], a lower activation energy value (~0.84 eV) was obtained for the vacancy binding energy of the stacking fault tetrahedron (SFT), in irradiations with fission neutrons at 220–450°C, at high damage rate 2×10^{-7} dpa s^{-1} and at a high fluence ~1.2 dpa. SFTs are the dominant vacancy cluster morphologies in Cu irradiated at 25°C and 200°C. This is quite different from fission neutron irradiation. In these cases, dislocation loops are prevalent at room temperature and SFT are observed mainly at elevated temperatures [18].

The isochronal recovery of the CRSS around Stage V ($T > 450$ K) in crystals irradiated at 300 K and at 77 K was studied in the present work. At low fluences, lower than 0.5×10^{21} n m^{-2} the CRSS is well defined [11,12,47], but at higher fluences an upper and a lower yield point was observed in the tensile tests [2].

The purpose of the first part of the present work was then to determine the neutron fluence $(\phi t)_C$ for which an upper and a lower yield point appear in Cu single crystals irradiated at 77 K, when tested at 77 K in a standard tensile test (hard machine).

Three specimens were irradiated at increasing fluences, starting with 0.5×10^{21} n m^{-2}. The choice of this value is due to the fact that in the microtensile machine (soft machine) [47,48] a sudden increase in the deformation rate was observed when neutron fluence was higher than 0.5×10^{21} n m^{-2} [49]. This increase was attributed to the presence of a lower yield point in a hard machine [47].

In Section 4.1 the following points are discussed:

- the choice of the upper yield point as the actual yield stress in the stress–strain curves when $\phi t > (\phi t)_C$, and
- the relation of the lower yield point with the formation of defect-free channels by sweeping of defect clusters by dislocations, i.e., dislocation channeling [7,50,51].

The purpose of the second part of the present work was the determination of the Stage V temperature range. Two series of experiments were performed in neutron irradiated Cu single crystals by isochronal recovery of the CRSS, measured at the reference temperature of 77 K. In the first series the conditions were irradiation temperature 300 K, and a fluence two orders of magnitude higher than $(\phi t)_C$. These experimental conditions reproduce those used in the few published papers in which similar techniques were used [1,43]. In the second series the conditions were 77 K and a fluence $\sim(\phi t)_C$.

To the authors' knowledge, isochronal recovery of radiation hardening has not been studied before under experimental conditions similar to those of the present work [1,35,43]. Some isothermal recovery determinations of neutron radiation hardening were performed in Cu in the temperature range 275–385°C by Makin [43,46,52] and by Blewitt et al. [1]. Both authors irradiated their specimens at ~30°C and high fluences ($>10^{22}$ n m^{-2}) and the tests were performed at 77 and 300 K.

The presence of inflections in the experimental curves, at 77 K and a fluence $\sim(\phi t)_C$, will be discussed in Section 4.2.

2. Experimental details

2.1. Production and preparation of specimens

Single crystal rods of 3 mm × 3 mm square cross-section, a gauge length of 30 mm and spherical heads 6.35 mm in diameter, were obtained for this study, by a modified Bridgman technique of gradual solidification from the melt [11,12], in vacuum. Specimens Cu-1, Cu-2 and Cu-3 were used for the determination of the critical fluence at which dislocation channeling is observed in Cu (see Table 1), and specimens Cu-4, 5, 6, 7, 8, 9 and 10 for the study of Stage V, respectively (see Table 2).

The specimens were prepared using 99.999% high purity copper rods supplied by Johnson–Matthey as starting material [18,53]. Three crystals of identical orientation were produced by solidification from a common seed. The back-reflection Laue method was used for determining crystal orientations ($\varepsilon \pm 1°$) (see Tables 1 and 2). These orientations were chosen in order to assure single slip when testing during isochronal annealing. 'As grown' single crystals, were strained about

Table 1
Pre- and post-annealing data of Cu specimens used for the determination of critical $(\phi t)_C$

Specimen	σ_0 (MPa)	χ_0 (degree)	λ_0 (degree)	Fluence ϕt (10^{20} m^{-2})	T_{irrad} (K)	σ_{00} (MPa) (upper yield point)
Cu-1	1.97	63	36	4.7	77	18.75
Cu-2	4.43	48	42	10	77	21.70
Cu-3	3.13	58	33	50	77	35.38

χ_0 and λ_0 are the angles, in the standard triangle, between the specimen axis and the pole (1 1 1) and $(\bar{1}\,0\,1)$, respectively.

Table 2
Pre- and post-annealing data of Cu specimens used for the determination of Stage V (runs 1–7)

Specimen	Runs	σ_0 (MPa)	χ_0 (degree)	λ_0 (degree)	Fluence ϕt (10^{20} m^{-2})	T_{irrad} (K)	σ_{00} (MPa) (upper yield point)
Cu-4	1	2.00	50	42	130	300	31.4
Cu-5	2	2.00	58	32	630	300	49.00
Cu-6	3	3.00	42	53	5.3	77	13.58
Cu-7	4	2.40	42	53	5.3	77	12.95
Cu-8	5	4.40	42	53	5.3	77	14.98
Cu-9	6	7.40 (*)	58	33	6.5	77	18.86
Cu-10	7	7.80 (*)	48	42	6.5	77	19.96

χ_0 and λ_0 are the angles, in the standard triangle, between the specimen axis and the pole (1 1 1) and $(\bar{1}\,0\,1)$ respectively. (*) Value of CRSS after doping of interstitial and vacancy loops.

1% during cooling from melting to room temperature, due to the lower expansion coefficient of graphite with respect to Cu. In order to get a lower pre-irradiation CRSS (σ_0) all the specimens were annealed during 3 h at 1170 K and 10^{-5} Torr [54]. The average value of σ_0 for the unirradiated specimens was consistent with values obtained by similar techniques in crystals of the same purity [55].

2.2. Neutron irradiation

The irradiation of the samples was performed in a cryostat [48], installed inside the core of the experimental reactor RA-1 at Comisión Nacional de Energía Atómica (CNEA). The reactor is a modified Argonaut type reactor, fueled with 20% enriched ^{235}U, light water moderated, used for basic research. The neutron spectrum in the irradiation chamber of the cryostat is typical of a research reactor: a thermal region of Maxwellian shape and a fast region of nearly fission shape ($E > 0.5$ MeV). The ratio of fast to thermal flux (ϕ_f/ϕ_{th}) is 1.3 [12,48,56]. Since the mean free path for fast neutron collisions with the lattice is about 20 mm in Cu, the ADCs are homogeneously distributed in the volume.

2.3. Annealing device

A device described elsewhere [36], was suitably modified in order to get temperature pulses between 77 and 800 K, in an inert pressurized atmosphere. The temperature pulses had thus a shorter rise time and they were equal in shape. The latter will allow us to take into account the specimen annealing before the final temperature T_a is reached. As shown in the insert of Fig. 1, each irradiated specimen (kept under liquid N_2) was first surrounded by a copper specimen temperature homogenizer, and then introduced inside a specimen chamber

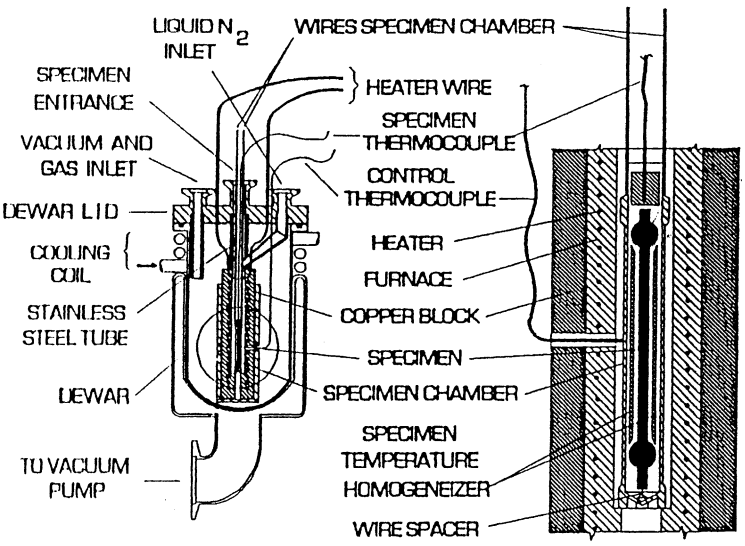

Fig. 1. Schematic diagram of the annealing device.

at 77 K. The latter was finally introduced into the furnace previously heated at the annealing temperature, T_a.

The specimen temperature was measured with a thermocouple, referred to as the specimen thermocouple, which is attached to a small copper block placed on the top and in close contact with the specimen. The furnace consists of an electrical resistance (heater wire) embedded in sprayed copper and surrounded by a copper cylinder (copper block). A control thermocouple is attached to the middle point of the heater. The location of the furnace inside the Dewar vessel is also shown in Fig. 1. The furnace is attached to the central inlet of the Dewar vessel lid (specimen entrance) by a stainless steel tube. The vessel lid is water cooled by a cooling coil. A second inlet (vacuum and gas inlet) in the lid allows evacuation and pressurizing of the chamber with inert gas to avoid oxidation of the specimen during annealing. Furnace cooling at the end of annealing is achieved by introducing liquid N_2 via a third inlet (liquid N_2 inlet). The metallic furnace has a low thermal inertia and a stability of the order of 0.1 K is achieved using a differential temperature controller. Heat convection is minimal since the specimen chamber is closed at the lower end and the gap between chamber and furnace is 0.25 mm. The specimen is therefore heated mainly by conduction since radiation is low at the Stage V temperatures. The transmission by conduction determines then the shape of pulses in the temperature range of Stage V. Fig. 2 shows the evolution of the specimen temperature during annealing at $T_a = 573$ K. Pulses shape could be described by the expression

$$T(t) = a[1 - \exp(-bt)] + c,$$

where c the temperature for $t = 0$, $a + c = T_a$ and $b^{-1} = \Gamma a$ characteristic rise time ($5\Gamma = 99\%T_a$). For the device shown in Fig. 1, 5Γ is equal to 3.5 min.

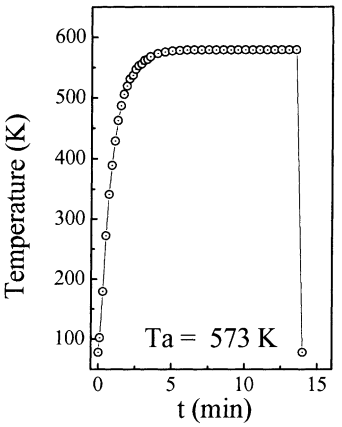

Fig. 2. Temperature pulse (77–573 K). Temperature falls sharply to 77 K after injection of liquid N_2.

2.4. Tensile tests

The out-of-pile tests were performed in an Instron tensile machine, model 4465, at a crosshead speed of 1.11×10^{-4} s^{-1}. The machine was fitted with an inverted device allowing the sample to be completely immersed in liquid nitrogen inside the Dewar vessel. A careful procedure allowed irradiated samples to be mounted and tested at 77 K avoiding any intermediate warming.

Fig. 3 shows the first part of the load–elongation curve of the as-irradiated specimen at a fluence close to $(\phi t)_C$, Cu-1, (see Table 1). The micro-strain region is wider (~0.54%) than the corresponding region of the unirradiated crystals ($\leqslant 0.1\%$) [57]. An enlargement of the macro-strain region (A–B) is shown in Fig. 4(a).

A hysteresis loop is always observed in this tensile machine when the sample is loaded and unloaded during the tensile test, since the crosshead speed is not a step function during the first seconds after the direction reversal. However, this is not relevant for the yield stress determination. Any possible accommodations of the grips during the tensile test are not relevant either.

The values of the post-irradiation CRSS, when $\phi t > (\phi t)_C$, correspond to the upper yield point, as will be discussed in Section 4.1.

2.5. Isochronal recovery of the CRSS

The isochronal annealing programs, after irradiations, were carried out using successive temperature pulses, and were indicated as 'runs 1–7' (see Table 2). In all cases the annealing time was 10 min, starting at the moment when the specimen reached a temperature five degrees below the annealing temperature T_a (see Fig. 2).

For each test of the runs 1–7, the yield stress value corresponds to an average macro-strain ~0.1% (point C in Fig. 3). Work hardening increases the yield stress and

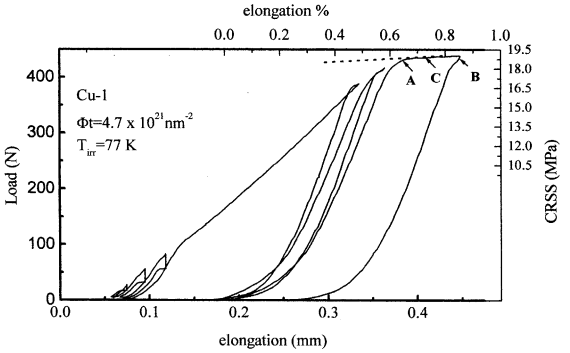

Fig. 3. The first part of the load–elongation curve measured at 77 K of Cu-1 single crystal neutron irradiated at 77 K and a fluence of 0.47×10^{21} n m^{-2}.

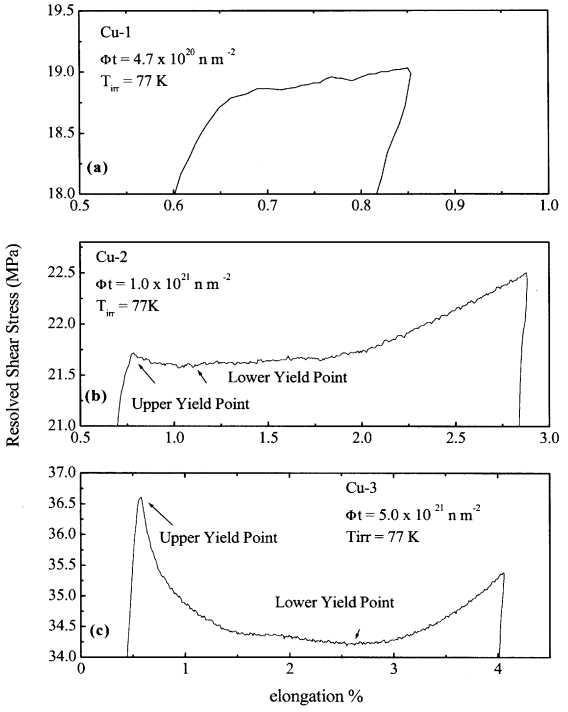

Fig. 4. The initial appearance of upper and lower yield points in Cu-1, Cu-2 and Cu-3 single crystals, irradiated and measured at 77 K and fluences $\sim(\phi t)_C$, $\sim 2(\phi t)_C$ and $\sim 10(\phi t)_C$. An enlargement of the corresponding first parts of the load–elongation curves is shown in (a)–(c).

some of the defects produced disappear in the next annealing. In order to evaluate how this small perturbation of the yield stress affects the temperature of the inflection in the isochronal annealing curves, the yield stress at the beginning of plastic strain (point A in Fig. 3), was also considered. However, the temperature corresponding to the inflection was the same.

For runs 3–5, the total strain at the end of the isochronal recovery program does not exceed 3%. Assuming homogeneous strain, the error in the value of the CRSS is negligible, since the rotation of the slip plane is small.

We define σ_{00} as the CRSS 'as-irradiated' value and σ^{T_a} as the CRSS measured after each temperature pulse T_a. A conventional method of plotting recovery rate data was used. The CRSS (σ^{T_a}) normalized to σ_{00}, was plotted vs. the annealing temperature T_a.

In order to show more clearly the temperatures at which inflections are present, in some cases the numerical derivatives are also plotted (rate curves). All recovery rate curves were computed by the expression

$$\tfrac{1}{2}([y_{i+1}-y_i]/[x_{i+1}-x_i]) + [y_i - y_{i-1}]/[x_i - y_{i-1}]).$$

It must be emphasized that the procedure is purely mathematical and does not include the application of any specific annealing kinetics. This method allows also a better comparison of the experimental data.

3. Results

3.1. The load–deformation curves near the upper and lower yield points: the critical fluence

In the determination of the fluence dependence of the CRSS with a soft machine, it was observed in every tensile test that plastic hardening rates decrease in Cu, Zn and Mg for increasing values of the fluence, reaching the value zero at $\sim(\phi t)_C$ [49]. Thus, it was decided to perform a series of irradiations at fluences higher than $(\phi t)_C$ in Cu in a hard machine.

In order to show the initial appearance of upper and lower yield points in Cu single crystals, specimens Cu-1, Cu-2 and Cu-3, were irradiated at 77 K and fluences $\sim(\phi t)_C$, $\sim 2(\phi t)_C$ and $\sim 10(\phi t)_C$, respectively, (see Table 1). An enlargement of the first part of the Resolver Shear Stress vs elongation % curve at 77 K is shown in Figs. 4(a)–(c). In Fig. 4(a) the CRSS is well defined. Fig. 4(b) shows the appearance of the lower yield point in the stress–strain curve. The difference in stress between the upper and the lower yield points is about 1%. It appears that the difference between the upper and the lower yield points increases with the fluence [1] and is about 5.5% in Fig. 4(c).

From these experimental results a critical fluence $(\phi t)_C$ of $\sim 0.5 \times 10^{21}$ n m^{-2} was adopted, which is in accordance with the following facts:

1. the onset of the yield point drop in Mg which was associated to the channeling phenomenon [11,47];
2. a total loss of ductility in Zn which was associated to channeling as well [11,12,58];
3. the departure from linearity of σ_i vs. $(\phi t)^{0.5}$ in Cu, Mg and Zn when the fluence dependence is measured in the same single crystal, [11,12,47], (σ_i is the CRSS which would be measured if the loops were the only barriers to the movement of dislocations).

This departure in Cu irradiated with neutrons is due to two main facts:

(a) loops swept by the passage of dislocations (dislocation channeling) [7];

(b) a change in the defects cluster production rate from linear to sublinear [17,35].

Zinkle results [25] show this change in Cu irradiated with neutrons of 14 MeV at a fluence of 3×10^{20} n m^{-2}.

The characteristics of the mechanical behavior of Cu, as compared with Mg and Zn, are discussed in Section 4.1.2.

3.2. Stage V

3.2.1. Specimens irradiated at 300 K and a fluence $\sim 20(\phi t)_C$

Fig. 5 shows the isochronal recovery during runs 1 and 2. The temperature range of Stage V is 500–650 K. For both runs, the peak is located at about 587 K and is asymmetrical. The shape suggests the presence of a not resolved substage, probably due to the ΔT chosen for these runs (~30 K). In run 1 there was some indication of a recovery peak. The aim of run 3 was to study this temperature range in more detail.

3.2.2. Specimens irradiated at 77 K and a fluence $\sim(\phi t)_C$

Stage V study was continued considering three temperature intervals, corresponding to specimens Cu-4, Cu-5 and Cu-6 (runs 3, 4 and 5) respectively. The specimens were identically prepared and simultaneously irradiated at $(\phi t)_C$, in the way described in Sections 2.1 and 2.2, respectively.

Fig. 6 (run 3) shows the isochronal recovery (9 experimental points) in the temperature range 490–520 K. An inflection located at ~505 K is observed. This value was coincident with the above-mentioned shoulder of run 1. In the present work this peak is designated V_a.

The isochronal recovery of the specimen Cu-4 of the run 4 in the temperature range 520–560 K is shown in

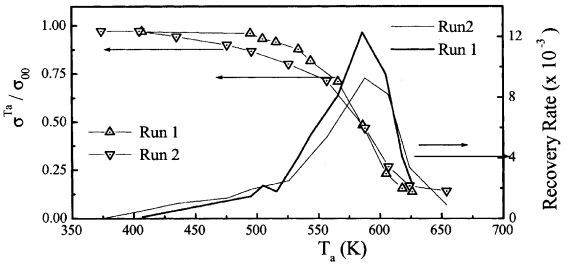

Fig. 5. Isochronal annealing (10 min) and recovery rate of Cu single crystals irradiated with neutrons at 300 K. △ Run 1, $\sigma_0 = 2.0$ MPa, $\phi t = 6.3 \times 10^{22}$ n m^{-2}, $\sigma_{00} = 49.0$ MPa. ▽ Run 2, $\sigma_0 = 2.0$ MPa, $\phi t = 1.3 \times 10^{22}$ n m^{-2}, $\sigma_{00} = 31.4$ MPa.

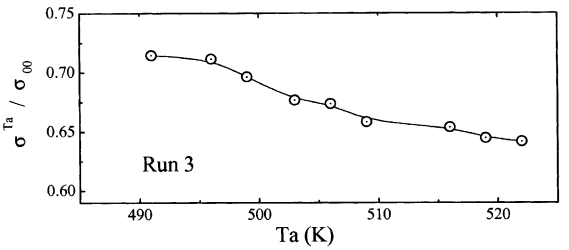

Fig. 6. Run 3, isochronal annealing (10 min) of Cu single crystals irradiated with neutrons at 77 K. $\sigma_0 = 3$ MPa, $\phi t = 5.3 \times 10^{20}$ n m^{-2}, $\sigma_{00} = 13.58$ MPa.

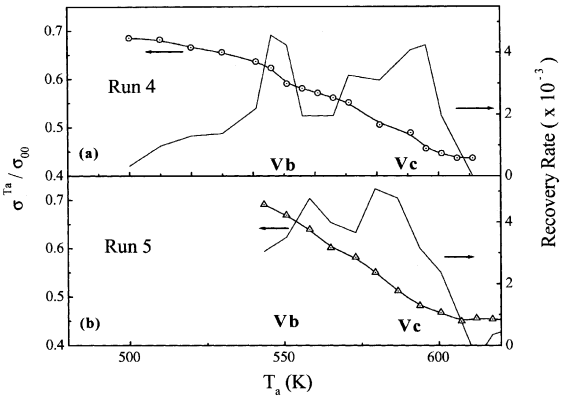

Fig. 7. Isochronal annealing (10 min) and recovery rate of run 4 and 5 of Cu single crystals. $\phi t = 5.3 \times 10^{20}$ neutrons m^{-2}, $T_{irr} = 77$ K. (a) Run 4, $\sigma_0 = 2.4$ MPa, $\sigma_{00} = 12.95$ MPa. (b) Run 5, $\sigma_0 = 4.4$ MPa, $\sigma_{00} = 14.98$ MPa.

Fig. 7(a). Two inflections are observed in the experimental curve. The V_a peak was not observed in this case since only three experimental points were measured in the temperaure subinterval 490–520 K. Both peaks of the recovery spectrum were designated in the present work as peaks V_b and V_c. The V_b peak is placed between ~540 and 560 K and the V_c peak is in the range ~560–610 K. The V_b peak, located at ~550 K, is narrow (half width ~12 K).

Fig. 7(b) shows the thermal recovery of the specimen of run 5. The recovery started at 540 K (near of the V_b peak) and shows the inflection corresponding to V_c peak (~587 K).

3.2.3. Doped specimens irradiated at 77 K and a fluence $\sim 1.3(\phi t)_C$

The dependence and reproducibility of the recovery spectrum observed in runs 3, 4 and 5 with the defect clusters was investigated with the specimens of runs 6 and 7. They were previously irradiated at 300 K and 6.5×10^{20} n m^{-2}, deformed ~3% at 77 K and annealed in vacuum (10^{-5} mm Hg) during 40 min at 700 K (50% melting temperature). In this way, thermally stable defect clusters, larger than those produced by low temperature irradiation, are partially retained (radiation doping). The value of CRSS, before the second irradiation was higher than the as-grown value and it is indicated with (*) in Table 2.

The isochronal recovery of run 6 was measured in the temperature range 77–620 K (31 experimental points). Fig. 8 shows only the isochronal recovery of Stage V (16 experimental points). The stage is located in the range 480–600 K and the peak is placed at 560 K.

Run 7 shows (see Fig. 9) the Stage V (28 experimental points); the inflections corresponding to the V_b and V_c peaks are in the temperature ranges ~500–550 K (V_b),

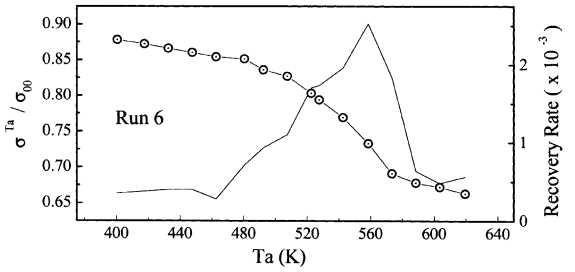

Fig. 8. Run 6 isochronal annealing (10 min) and recovery rate of the Cu single crystal with radiation doping, $\sigma_0 = 2.5$ MPa, $T_{irr} = 77$ K, $\phi t = 6.5 \times 10^{20}$ n m^{-2}, $\sigma_{00} = 18.86$ MPa.

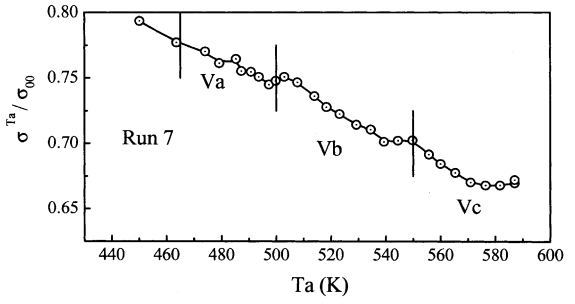

Fig. 9. Run 7, isochronal annealing (10 min) and recovery rate of the Cu single crystal with radiation doping, $\sigma_0 = 2.5$ MPa, $T_{irr} = 77$K, $\phi t = 6.5 \times 10^{20}$ n m^{-2}, $\sigma_{00} = 19.96$ MPa.

and 550–600 K (V_c). The peaks in Fig. 9 are located at 528 and 563 K, respectively. The onset of V_a peak (450–500 K) is not clearly defined due to the low number of experimental points in the range 420–480 K (3 points).

Fig. 10 shows some of the successive tensile tests of the isochronal annealing of run 7 in the temperature range of the V_b peak. At $T = 497$, 500 and 503 K a yield stress increase is observed because recovery is smaller than work hardening. At 539, 544, 549 K, the yield stress

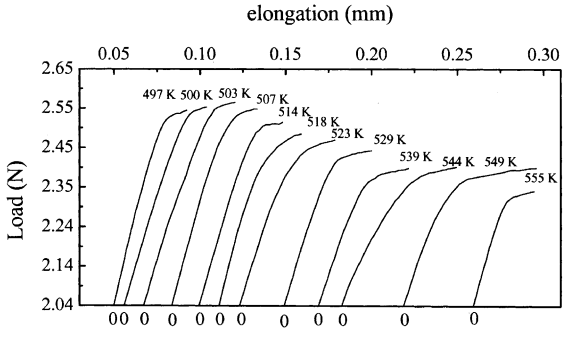

Fig. 10. Tensile tests performed after different temperature pulses, indicated on each load–elongation curve, in the temperature range of substage V_b (run 7).

values are approximately equal. In the following recovery at 555 K the yield stress was appreciably lower for the same temperature increase than the last recovery at 549 K.

Comparing the different runs, it could be seen that:

- The peak of Stage V (587 K) corresponding to runs 1 and 2 irradiated at 300 K and moderate fluences is coincident with the V_c peak of runs 4 and 5 irradiated at low fluences at 77 K. The final temperature of Stage V (~640 K) for the specimens of runs 1 and 2 is extended about 30 K towards higher temperatures, as compared with runs 4 and 5.
- For runs 6 and 7 (with radiation doping and after irradiation at low fluences 6.5×10^{20} n m^{-2} at 77 K) there is a shift of the peaks of about 20 K towards lower temperatures as compared with runs 4 and 5.
- For runs 6 and 7 the value of the relationship between the CRSS at the end of Stage V ($\sigma^{600\ K}$) and the as-grown CRSS is ~2.3 times larger than that corresponding to other runs.

4. Discussion

4.1. Critical fluence and the actual yield stress

4.1.1. At $\phi t < (\phi t)_C$

For fluences lower than $(\phi t)_C$ the stress–strain curves for single crystals of Mg, Zn and Cu irradiated and measured at 77 K show no particular features [11,12,47]; this can be considered as the standard behavior of plastic deformation. Then, the vacancy loops created by fast neutron irradiation are stable during plastic deformation.

4.1.2. At $\phi t > (\phi t)_C$

For fluences higher than $(\phi t)_C$, a different mechanical behavior is observed in Cu, Mg and Zn under plastic deformation. During tensile testing of Cu single crystals, the load elongation curve shows an upper and lower yield point. We consider that the value of the upper yield point is more representative of the actual yield stress than the lower yield point. The lower yield point is a consequence of the dislocation channeling. An example which supports even more the choice of the actual yield stress and the beginning of dislocation channeling at fluence $(\phi t)_C$ was found in Mg and Zn when each measurement of the CRSS vs ϕt was performed using different single crystals (as opposed to the determination of the fluence dependence where the same single crystal was tested in a soft machine [11,47]), that is:

- in Mg, the fluence dependence of the upper yield point, with power 0.5 of the fluence extends up to 3×10^{21} n m^{-2} [11,59],
- in Zn single crystals there is a complete ductility loss: the specimen fractures after a very low plastic defor-

mation (<0.1%) [11,12]. If we consider the yield point coincident with the fracture load, the calculated CRSS follows a 0.5 power law with the fluence up to 1.2×10^{21} n m^{-2} [11,49]. For $\phi t < (\phi t)_C$ the plastic strain at fracture lies between 3.7% and 6.8% [11,12,49] not depending on the fluence. Consequently the fracture mechanism does not change for this condition.

In previous papers, the different plastic behavior of Zn and Mg was attributed to dislocation channeling for $\phi t \geqslant (\phi t)_C$ [12,47,49].

Thus, the dislocation channeling phenomenon in Cu begins at $\phi t \geqslant (\phi t)_C$ and is coincident with the onset of the lower yield point. In a previous work [2] the upper yield point was attributed to a local stress magnification introduced by the advancing front of the Lüders bands, and when homogeneous strain is achieved, a representative yield stress could then be computed. However, the above-mentioned arguments, led us to consider that the upper yield point should be adopted as the actual yield point.

4.1.2.1. Comparison of mechanical properties of Cu and Mg under irradiation. The difference in the plastic behavior of Cu (absence of stress drop points) and Mg specimens (with stress drop points), which are both ductile, could be explained as follows. In Mg each stress drop is associated to the formation of slip packets, 0.5 mm apart, produced by sweeping of vacancy loops [47,48]. In Cu the size of the defect clusters is larger than in Mg [14–16,58,59]. Then, the higher stability of vacancy loops in Cu with respect to the dislocation movement explains the absence of stress drops. On the other hand, in Cu (fcc) there are four available close-packed glide planes as compared with only one in Mg (hcp). Consequently, in the former, the sweeping process by dislocations involves less vacancy loops than in the latter, and thus 'work softening' in Cu is less pronounced than in Mg.

4.1.2.2. Comparison of mechanical properties of Cu and Zn under irradiation. Since the size of the dislocation loops in Zn and Cu is similar [14,16,58,59], the difference in the plastic behavior of Cu and Zn specimens could be explained taking into account their different ductility. The ductility of Zn ($\Delta l/l_0 \sim 4\%$) is fluence independent for fluences lower than $(\phi t)_C$ [11,12,58], and is very low when compared with that of Cu. For fluences higher than the critical fluence, the rupture strain for Zn is reached in the activated slip packets due to dislocation channeling, before any other possible slip packet can be activated, as opposite to the case of Cu.

4.2. Recovery of stage V

4.2.1. Runs 1 and 2 irradiated at 300 K and a fluence $\sim 20(\phi t)_C$

In order to study Stage V in Cu, our determinations were performed in the range 450–620 K. This interval is different from that used by Diehl et al. [35]. In these experiments the isochronal recovery was interrupted at 450 K (Stages I, II and III), corresponding to a hardening recovery of 25% of the 'as irradiated' value in Cu neutron irradiated at 20 K. Consequently, the remnant hardening (75%), takes place mostly in Stage V. Fluences similar to those employed in the first part of this work (runs 1 and 2), were used by Blewitt et al. [1] and Makin et al. [43]. They were interested in the phenomenological determination of the activation energy of Stage V in copper by isothermal annealing of the yield stress at deformation temperatures of 78 and 300 K. In the experimental conditions of the present work ($\sim 10^{22}$ n m^{-2} at 300 K), both interstitial and vacancy loops are produced [43].

Stage V dependence with the fluence is shown by the increasing size of the recovery peak areas and their shift towards higher temperatures.

For the same experimental conditions Shimomura et al. [60] have observed by TEM the simultaneous disappearance of vacancy and interstitial loops by evaporation of vacancies from the vacancy loops and their annihilation at the interstitial loops.

4.2.2. Runs 3, 4, and 5 irradiated at 77 K and a fluence $\sim(\phi t)_C$

Our results in Cu at low fluence and temperature reveal the presence of a broad recovery stage. Initial results suggest the presence of three recovery substages located in the ranges ~490–520, ~520–560 and ~560–620 K, respectively. The substages observed in the recovery of the CRSS were not observed by electrical resistivity measurements [1]. We consider that the relatively low sensitivity of electrical resistivity to the characteristics of defect clusters prevents the detection of this sub-structure. In the specimens used in runs 3–5, Frank vacancy dislocation loops are produced [14,17]. The dispersion of their diameters is small [27,28,61,62], and they are thermally stable up to the beginning of Stage V [63,64]. During irradiation there is neither overlap nor uncorrelated interstitial atoms recombination between neighboring cascades. This is due to the fact that the average distance between ADCs is larger than the average range of dynamical crowdions [24,35]. A progressive disappearance of small clusters in the temperature range ~490–520 K (V_a peak) was observed by TEM by Shimomura et al. [60], in Cu irradiated at 2.7×10^{21} n m^{-2} and 350 K. This peak can be associated to the recovery of vacancy clusters of low thermal stability nucleated above Stage III. This assumption is

consistent with the result of Schilling et al. [30], in electron irradiated Cu. Some recovery of the electrical resitivity was observed by these authors in the temperature range ~490–520 K (V_a peak). In the temperature range ~520–620 K (runs 4 and 5), Shimomura et al. [60] observed the simultaneous disappearance of vacancy and interstitial clusters. At ~620 K they observed that only vacancies were dissolved. Diverse complementary techniques in the same experimental conditions are required to obtain the data, which lead to an explanation of the underlying mechanisms responsible for the recovery spectrum observed. The determinations of isochronal recovery in Cu in the range of Stage V employing positron annihilation [60] or perturbed $\gamma\gamma$ angular correlation technique (PAC) [40] give peaks coincident with our results.

4.2.3. Runs 6 and 7 irradiated 77 K and a fluence ~1.3$(\phi t)_C$

Stage V corresponding to the specimens with 'radiation doping' (runs 6 and 7) shows a shift of ~20 K towards lower temperatures, as compared with the corresponding peaks of the 'as-grown' specimens. A small shift of Stage V was also observed by electrical resistivity determinations [44].

The remnant hardening in the samples used in runs 6 and 7 was higher than in the 'as-grown samples' corresponding to other runs due to the following facts.

We define $\sigma_i^{T_a}$, which is only due to the interaction of the moving dislocations with the vacancy dislocation loops population modified by the temperature pulse. In order to know $\sigma_i^{T_a}$ for single crystals used in runs 6 and 7, we must know the additivity law of the stress corresponding to the large loops (doping) with the vacancy dislocation loops population modified by the temperature pulse and the athermal stress of the single crystal [11,12,47,65]. In simple cases such as 'as-grown' irradiated Cu single crystals, Runs 1–5, the CRSS is $\sigma_i^{T_a} = \sigma^{T_a} - \sigma_0$. In predeformed and irradiated Cu single crystals $\sigma_i^{T_a} = \sigma^{T_a} - (\sigma_0)_{ath}$, where $(\sigma_0)_{ath}$ is the athermal component of σ_0.

For the single crystals used in runs 6 and 7, neither the additivity law nor the athermal component of the CRSS are known. If the $\sigma_i^{T_a}$ vs T_a curve could be represented, the difference in the remnant hardening would be minimal.

5. Conclusions

From the present work on neutron-irradiated Cu single crystals, it can be concluded that:

Defect clusters produced by neutron irradiation at 77 K and a fluence lower than 0.5×10^{21} n m^{-2} are stable during plastic deformation. This value was considered to be the critical fluence $(\phi t)_C$.

The dislocation channeling phenomenon in Cu begins at $\phi t \geqslant (\phi t)_C$ and is coincident with the appearance of the lower yield point. The upper yield point is adopted as the actual yield point.

A broad recovery stage between 500 and 650 K corresponding to stage V was determined.

The presence of inflections in the Stage V in the isochronal curves at 77 K, suggests the presence of three substages in Cu neutron irradiated at 77 K at fluences close to the critical fluence $\sim(\phi t)_C$.

Acknowledgements

The authors are very pleased to express their gratitude to Mr C.D. Anello for his collaboration in the construction of the annealing equipment and assistance during the irradiation experiments, and to the Radiation Damage Group for their invaluable help. The cooperation of the personnel of CNEA-RA-1 Reactor and Materials Department is gratefully acknowledged. The authors would also like to thank Dr M. Ipohorski and Mr A.M. Hey for their interest.

References

[1] T.H. Blewitt, R.R. Coltman, R.E. Jamison, J.K. Redman, J. Nucl. Mater. 2 (1960) 277.
[2] T.H. Blewitt, in: D.S. Billington (Ed.), Proceedings of the International School of Physics 'Enrico Fermi' XVIII Course: Radiation Damage in Solids, Academic Press, New York, London, 1962, p. 630.
[3] A. Seeger, U. Essmann, in: D.S. Billington (Ed.), Proceedings of the International School of Physics 'Enrico Fermi' XVIII Course: Radiation Damage in Solids, Academic Press, New York, London, 1962, p. 717.
[4] J. Diehl, Radiation damage in solids, in: Int. Atomic Energy Agency Vienna, 1962, p. S129.
[5] R.L. Fleicher, Acta Metall. 10 (1962) 835.
[6] R.L. Fleicher, J. Appl. Phys. 33 (1962) 3504.
[7] J.V. Sharp, Philos. Mag. 16 (1967) 77.
[8] P.M. Kelly, Int. Metall. Rev. 18 (1973) 31.
[9] U.F. Kocks, Mater. Sci. Eng. 27 (1977) 291.
[10] K. Shinohara, S. Kitajima, J. Nucl. Mater. 133–134 (1985) 690.
[11] H.C. González, PhD thesis, Inst. Balseiro, Univ. Nac. de Cuyo, Argentina, 1973.
[12] H.C. González, E.A. Bisogni, Phys. Status Solidi (a) 62 (1980) 351.
[13] D.S. Billington, J. Crawford, Radiation Damage in Solids, Princeton University, Princeton, NJ, 1961, p. 115.
[14] J.A. Brinkman, J. Appl. Phys. 25 (1954) 961.
[15] J.A Brinkman, Am. J. Phys. 24 (1956) 246.
[16] J.A. Brinkman, Fission Damage in Metals Rendiconti della Scuola Internazionale de Fisica 'E. Fermi', Academic Press, New York, 1962, p. 630.

[17] A. Seeger, in: Proceedings of the Second International Conference on The Peaceful Uses of Atomic Energy, vol. 6, United Nations, New York, 1958, p. 250.
[18] N. Yoshida, Y. Akashi, K. Kitajima, M. Kiritani, J. Nucl. Mater. 133&134 (1985) 405.
[19] R. Rauch, J. Peils, A. Schumalzbauer, G. Wallner, J. Nucl. Mater. 168 (1989) 101.
[20] M. Kiritani, T. Yoshiie, S. Kojima, Y. Satoh, K. Hamada, J. Nucl. Mater. 174 (1990) 327.
[21] R. Rauch, J. Peils, A. Schumalzbauer, G. Wallner, J. Phys. Condens. Mater. 2 (1990) 9009.
[22] J. Peisl, H. Franz, A. Schumalzbauer, G. Wallner, Mater. Res. Soc. Symp. Proc. 209 (1991) 271.
[23] H. Wiederich, J. Nucl. Mater. 206 (1993) 121.
[24] R.S. Averback, T. Diaz de la Rubia, in: H. Ehrenreich, F. Spaepen (Eds.), Displacement Damage in Irradiated Metals and Semiconductors, Solid State Physics, vol. 51, Academic Press, New York, 1998, p. 281.
[25] S.J. Zinkle, Radiat. Eff. Def. Solids 148 (1999) 447.
[26] Landølt-Börnstein, Zahlenwert und Funktionen aus Naturwissenschaften und Technik, Band 25 Atomare Fehlstellen in Metallen, Springer, Berlin, 1994, p. 233.
[27] C.A. English, J. Nucl. Mater. 108–109 (1982) 104.
[28] B.L. Eyre, J. Phys. F 3 (1973) 423.
[29] H.R. Brager, F.A. Garner, N.F. Panayotou, J. Nucl. Mater. 103&104 (1981) 995.
[30] W. Shilling, G. Burger, K. Isebeck, H. Wenzl, in: A. Seeger, D. Schumacher, W. Schilling, J. Diehl (Eds.), Annealing Stages in The Electrical Resistivity of Irradiated FCC Metals, North-Holland, Amsterdam, 1969, p. 255.
[31] W. Schilling, K. Sonnenberg, J. Phys. F 3 (1973) 322.
[32] F.W. Young Jr., in: N.L. Petersen, S.D. Harkness (Eds.), Defect Annealing Processes in Metals, American Society for Metals, Metals Park, OH, 1976, p. 95.
[33] F. Pleiter, C. Hohenemser, Phys. Rev. B 25 (1982) 106.
[34] P. Ehrhart, K.H. Robrock, H.R. Schober, in: R.A. Johnson, A.N. Orlov (Eds.), Basic Defects in Metals, vol. 13, North-Holland, Amsterdam, 1986, p. 60.
[35] J. Diehl, Ch. Leitz, W. Schilling, Phys. Lett. 4 (1963) 236.
[36] H.C. González, C.J. Iriart, Philos. Mag. A 54 (1986) 441.
[37] J. Nihoul, Phys. Status Solidi 3 (1963) 2061.
[38] R.R. Coltman, C.E. Klabunde, J.K. Redman, Phys. Rev. 156 (1967) 715.
[39] J.A. Horak, T.H. Blewitt, J. Nucl. Mater. 49 (1973/74) 161.
[40] T.H. Wichert, Mater. Sci. Forum 15–18 (1987) 429.
[41] H. Fukuyama, Y. Shimomura, M.W. Guinan, J. Nucl. Mater. 155–157 (1988) 1205.
[42] B.N. Singh, S.J. Zinkle, J. Nucl. Mater. 206 (1993) 212.
[43] M.J. Makin, S.A. Manthorpe, Philos. Mag. 10 (1964) 580.
[44] W. Schilling, P. Ehrhart, K. Sonnenberg, in: M.T., Robinson, F.W. Young, Jr., (Eds.), Fundamental Aspects of Radiation Damage in Metals, ERDA Conf. 751006, vol. 1, National Technical Information Service, Springfield, Virginia, US Deparment of Commerce, 1976, p. 470.
[45] M.T. Miralles, A.M. Fortis, H.C. González, An. Asoc. Qca Arg. 84 (1996) 429.
[46] M.J. Makin, in: W.F. Sheely (Ed.), Radiation Effects, Metallurgical Society Conf., vol. 37, Gordon and Breach, New York, 1967, p. 627.
[47] H.C. González, Phys. Status Solidi (a) 86 (1984) 169.
[48] H.C. González, T.H. Blewitt, E.A. Bisogni, Micromáquina de Tracción y Criostato que Operan en el Reactor RA-1, CNEA-NT29-76, 1976.
[49] H.C. González, unpublished results.
[50] A.H. Cottrell, Vacancies and Other Point Defect in Metals, London, 1958, p. 1.
[51] I.G. Greenfield, H.G.F. Wildsdorf, J. Appl. Phys. 32 (1961) 827.
[52] M.J. Makin, S.A. Manthorpe, Philos. Mag 8 (1963) 1725.
[53] D.G. Martin, Philos. Mag. 7 (1962) 803.
[54] J.H. Wernick, H.M. Davis, J. Appl. Phys. 2 (1956) 149.
[55] T.H. Blewitt, Phys. Rev. 91 (1953) 1115.
[56] Bovisio de Ricabarra, Departamento de Reactores, Centro Atómico Constituyentes (CAC), Comisión Nacional de Energía Atómica (CNEA, 1968), private communication.
[57] T.H. Blewitt, C.A. Arenberg, Suppl. Trans. JIM 9 (1968) 226.
[58] C.J. Iriart, A.M. Fortis, H.C. González, Acta Metall. 32 (1984) 389.
[59] H.C. González, C.J. Iriart, Philos. Mag. A. 52 (1985) 243.
[60] Y. Shimomura, H. Fukushima, M. Kami, T. Yoshiie, H. Yoshida, M. Kiritani, J. Nucl. Mater. 141–143 (1986) 846.
[61] T.H. Blewitt, T.J. Koppenaal, Radiation Effects in Metals, AIME SEMIN, Asheville, NC, 1965.
[62] S.J. Zinkle, J. Nucl. Mater. 150 (1987) 140.
[63] G. Burger, H. Meissner, W. Schilling, Phys. Status Solidi 4 (1964) 267.
[64] T.H. Blewitt, T.L. Scott, R.A. Conner Jr., J. Nucl. Mater. 108&109 (1982) 442.
[65] J. Diehl, G.P. Seidel, in: Symposium on Radiation Damage in Reactor Material, IAEA., Vienna, June 2–6 1969, p. 187.